Electric Power Systems Research 123 (2015) 128–136

Contents lists available at ScienceDirect

Electric Power Systems Research

journal homepage: www.elsevier.com/locate/epsr

FDTD simulation of direct lightning strike to a phase conductor: Influence of corona on transient voltages at the tower

Tran Huu Thang[a], Yoshihiro Baba[b,*], Naoto Nagaoka[b], Akihiro Ametani[b], Naoki Itamoto[c], Vladimir A. Rakov[d]

[a] Tsuruoka National College of Technology, Department of Electrical and Electronic Engineering, Yamagata 997-8511, Japan
[b] Doshisha University, Department of Electrical Engineering, Kyoto 610-0321, Japan
[c] Hokuriku Electric Power Company, Institute of Research and Development, Toyama 930-8686, Japan
[d] University of Florida, Department of Electrical and Computer Engineering, Gainesville, FL 32611, USA

ARTICLE INFO

Article history:
Received 21 July 2014
Received in revised form 23 January 2015
Accepted 11 February 2015
Available online 6 March 2015

Keywords:
Lightning
Corona discharge
Finite-difference time-domain method
Transient voltage
Shielding failure

ABSTRACT

In this paper, a simplified model of corona discharge for the finite-difference time-domain (FDTD) computations has been applied to analysis of transient voltages at the tower of a transmission line caused by direct lightning strikes to an upper phase conductor. In the simulations, three 40-m towers, separated by 300 m, with one overhead ground wire and three phase conductors are employed. Corona is assumed to occur only on the upper phase conductor struck by lightning. The progression of corona streamers from the conductor is represented as the radial expansion of cylindrical conducting region around the conductor. The reduction of transient-voltage peak due to corona is not very significant, so that the voltage at the nearest tower exceeds the insulation level of 66/77 kV power line considered in this paper. For a 10-kA peak current, the upper-phase-conductor voltage peaks are reduced by 26% and 21% for a positive stroke with 1-μs- and 3-μs-risetime currents, respectively, and those for negative-stroke case are reduced by 18% and 13%, respectively. For a 20-kA peak current, the corresponding upper-phase-voltage peaks are reduced by 32% and 25% for the positive-stroke case, and those for the negative-stroke case are reduced by 22% and 15%.

1. Introduction

In our previous study, a simplified (engineering) model of corona discharge developed in Thang et al. [1,2] for the finite-difference time-domain (FDTD) computations (Yee [3]) has been applied to analysis of transient voltages at the tower of a 60-m-high transmission line, the ground wire of which is struck by lightning, and transient voltages computed with and without corona on the ground wire are compared. It is clear from the results of Thang et al. [4] that the transient voltages are reduced by corona discharge on the ground wire, but the reduction of transient-voltage peak is not very significant: the upper-, middle-, and lower-phase-voltage peaks are reduced by 15, 14, and 13% for a positive stroke with 50-kA-peak and 3-μs-risetime current, and those for a negative stroke with the same current waveform parameters are reduced by 10, 9, and 8%, respectively.

In this paper, we apply the same simplified model of corona discharge to the analysis of transient voltages of a 40-m tower for the case of direct lightning strikes to an upper phase conductor, at the midpoint of the span (shielding failure). Corona is assumed to occur only around the conductor struck by lightning. On the basis of the computed results, the effect of corona on transient voltages at the tower is examined. Note that the transient voltage is defined in this paper as the voltage between the phase conductor and the middle tower (no insulator is considered in the FDTD simulations). The objective here is to see if corona can reduce direct-strike overvoltages below the insulation level of the line.

The validity of the corona model of Thang et al. [1,2] has been tested against experimental data found in Noda [5], Noda et al. [6], Inoue [7], and Wagner et al. [8]. Specifically, it has been shown in [1] that the waveform of radial corona current, and the relation between the total charge (charge deposited on the wire and emanated corona charge) and applied voltage (q–V curve), computed using the FDTD method including the corona model for 22 m and 44 m long horizontal wires, agree reasonably well with the

* Corresponding author. Tel.: +81 774 65 6352; fax: +81 774 65 6801.
E-mail addresses: thangth@tsuruoka-nct.ac.jp (T.H. Thang), ybaba@mail.doshisha.ac.jp (Y. Baba), n.itamoto@rikuden.co.jp (N. Nagaoka), aametani@mail.doshisha.ac.jp (A. Ametani), rakov@ece.ufl.edu (V.A. Rakov).

http://dx.doi.org/10.1016/j.epsr.2015.02.006
0378-7796/

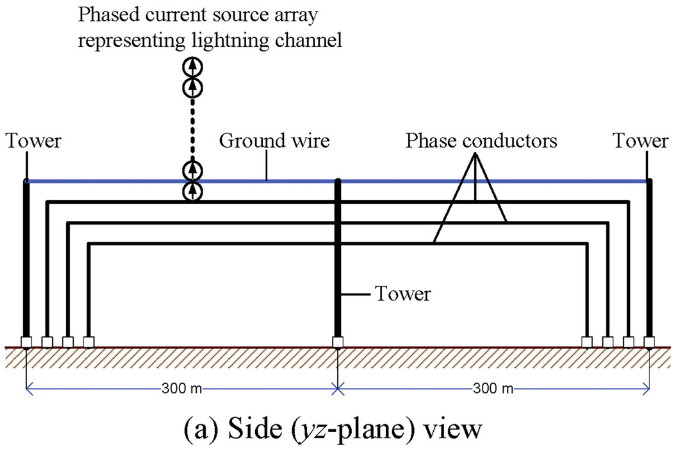

Fig. 1. Configuration of a two-span, 40-m high transmission line, analyzed using the FDTD method.

corresponding measured ones. Also, it has been shown in [1] that the computed increase of coupling between the energized wire and another wire nearby due to corona discharge agrees well with the corresponding measured one. Further, it has been shown in [2] that computed waveforms (including wavefront distortion and attenuation at later times) of fast-front surge voltages at different distances from the energized end of 1.4-km and 2.2-km long overhead wires agree reasonably well with the corresponding measured waveforms.

2. Methodology

The FDTD method involves the space and time discretization of the working space and the finite-difference approximation to Maxwell's equations. For the analysis of the electromagnetic response of a structure in an unbounded space using the FDTD method, an absorbing boundary condition, which suppresses unwanted reflections, is applied. The method requires the whole working space to be divided into cubic or rectangular cells. More details about the FDTD method and its application to lightning electromagnetic field and surge simulations are found in Baba and Rakov [9].

Fig. 1 shows the configuration considered in this paper. It is composed of three two-circuit 40-m towers, one overhead ground wire and three phase conductors (only one of the two circuits is

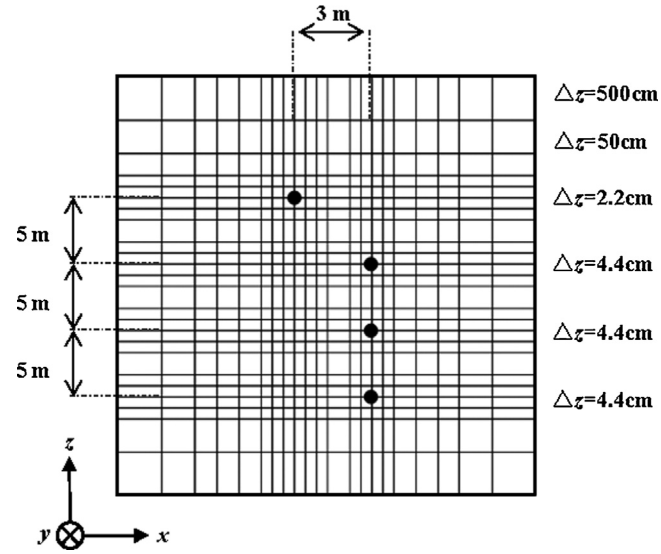

Fig. 2. Cross-sectional (zx-plane) view of the discretized space around horizontal conductors used in the FDTD computations.

considered). The separation distance between neighboring towers (span) is set to 300 m. This configuration is characteristic of real 66/77 kV transmission lines in Japan. Lightning is assumed to terminate at the midpoint of the upper phase conductor.

Each tower is represented by a 40-m high rectangular prism of cross-sectional area 2 m × 2 m, which includes a 5-m thick resistive (10-Ω) element of cross-section 2 m × 2 m and conductivity 0.125 S/m connected to the surface of a flat, perfectly conducting

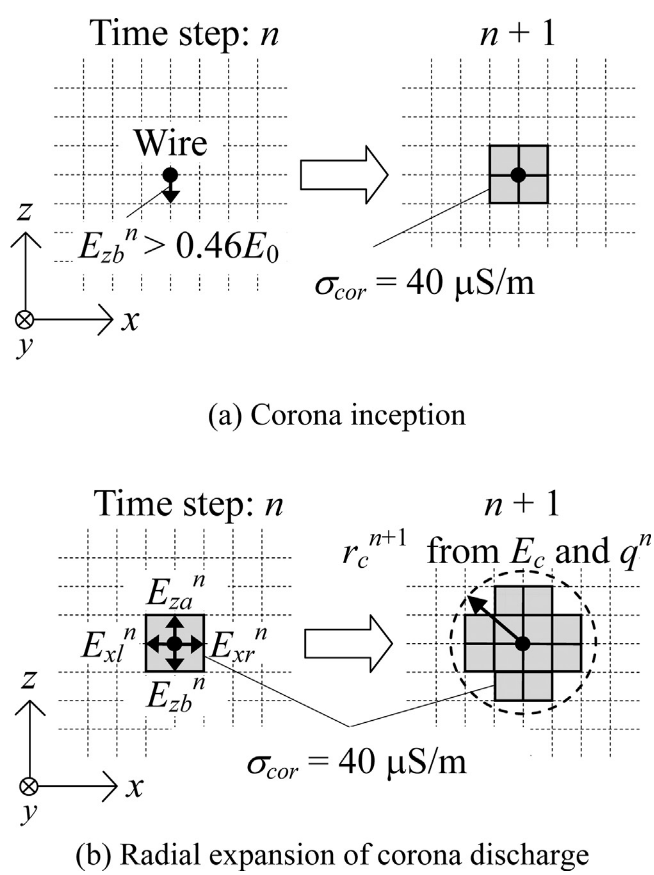

Fig. 3. FDTD representations of (a) inception of corona discharge at the wire surface and (b) radial expansion of corona discharge.

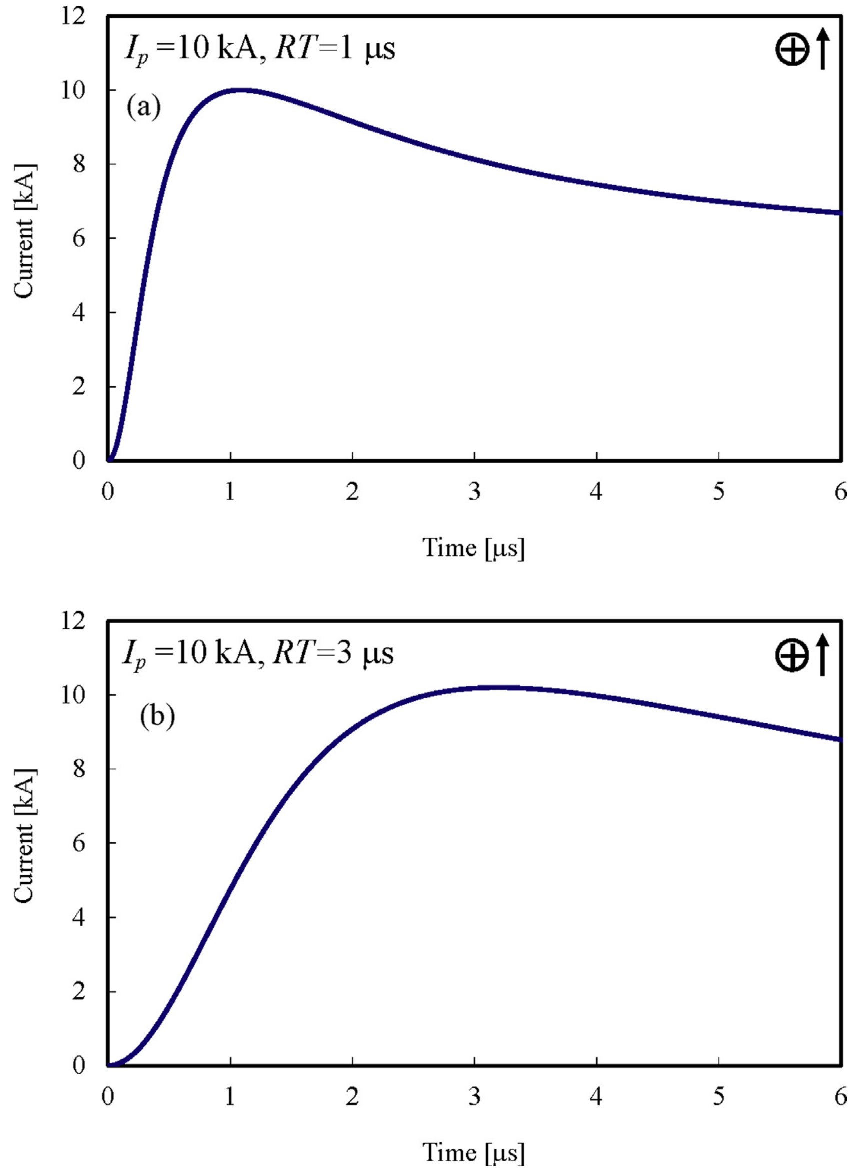

Fig. 4. Waveforms of injected negative lightning current (positive charge moving up. The peak of the injected current, I_p, is 10 kA, and its risetime, RT, is (a) 1 μs and (b) 3 μs.

ground. Each tower is connected to a single horizontal ground wire of radius 5 mm at its top. Upper-, middle-, and lower phase conductors have a radius of 10 mm and are suspended at heights of 35, 30, and 25 m, respectively, from the ground surface, and horizontally 3 m away from the axis of the tower (2 m from the tower surface). At each external tower (see Fig. 1a), the end of each phase conductors is connected to the ground via a vertical conductor and a matching resistor (530, 520, and 510 Ω for upper, middle, and lower phase conductors, respectively). The total length of the ground wire and each of the phase conductors is about 600 m. The lightning channel is represented by a 700-m long, vertical phased ideal current source array (Baba and Rakov [10]). The array simulates a current pulse that propagates upward at speed 130 m/μs, and its equivalent impedance is equal to infinity.

For FDTD computations, this conductor system is accommodated in a working volume of 60 m × 700 m × 900 m, which is divided nonuniformly into rectangular cells and is surrounded by five planes (the top plane and four side planes) of Liao's second-order absorbing boundary condition (Liao et al. [11]) to minimize unwanted reflections there. The bottom plane is set to a perfect conductor. The side length in y-direction of all the cells is 1 m (constant). Cell sides along x and z axes are not constant: 2.2 cm in the vicinity (2 cells × 2 cells = 4.4 cm × 4.4 cm) of the ground wire, 4.4 cm in the vicinity (20 cells × 20 cells = 88 cm × 88 cm) of each of the horizontal phase conductors, and increasing gradually to 50 and 500 cm beyond that region, as shown in Fig. 2. It has been shown by Noda and Yokoyama [12] that a zero-radius wire simulated by forcing the tangential components of electric field along the axis of the wire to zero has an equivalent radius of $0.23\Delta x$ or $0.23\Delta z$ (Δx and Δz are the side lengths of the square face, perpendicular to the wire, of rectangular cells used in the FDTD computations). Therefore, the equivalent radii of the horizontal wires used in this paper are $r_0 \approx 5$ mm ($= 0.23\Delta x = 0.23\Delta z = 0.23 \times 2.2$ cm) for ground wire and 10 mm ($= 0.23\Delta x = 0.23\Delta z = 0.23 \times 4.4$ cm) for phase conductors, respectively. The time increment is set to 0.047 ns, which is determined from the Courant stability condition for the smallest cell employed (2.2 cm × 1 m × 2.2 cm). Note that the use of smaller time increment, 0.0235 ns, does not cause any significant difference in computed results. Corona discharge is assumed to occur only on the upper-phase conductor.

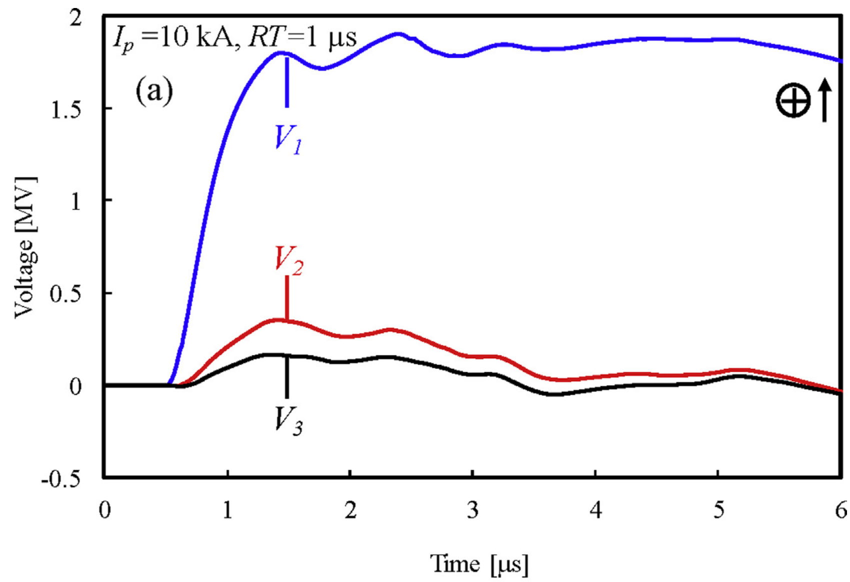

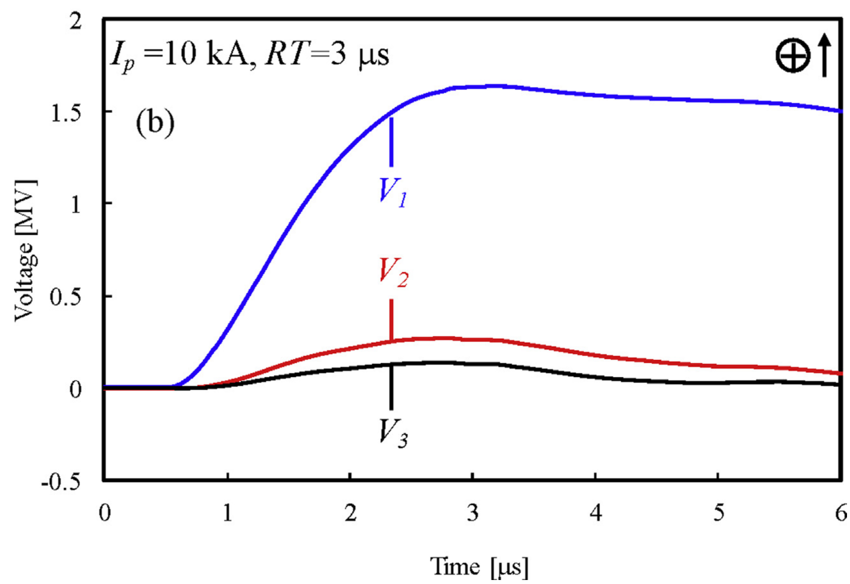

Fig. 5. FDTD-computed (for σ_{cor} = 40 μS/m, E_0 = 2.5 MV/m, and E_{cn} = 1.5 MV/m) waveforms of upper-, middle-, and lower phase transient voltages (V_1, V_2, and V_3, respectively) at the middle tower for a 10-kA negative lightning (positive charge moving up) with a current risetime of (a) 1 μs and (b) 3 μs.

We assume that the critical electric field E_0 on the surface of cylindrical conductor of radius r_0 for initiation of corona discharge is given by equation of Hartmann [13], which is reproduced below:

$$E_0 = m \times 2.594 \times 10^6 \left(1 + \frac{0.1269}{r_0^{0.4346}}\right) \quad [\text{V/m}] \tag{1}$$

where m is a coefficient depending on the conductor surface conditions. We assume that m = 0.5. When r_0 = 10 mm, E_0 is 2.5 MV/m for m = 0.5.

We set the critical background electric field necessary for streamer propagation (e.g., Cooray [14]) to E_{cp} = 0.5 MV/m for positive and E_{cn} = 1.5 MV/m for negative polarity (Waters et al. [15]). The corona ionization process is simulated by expanding the conducting region of constant conductivity (σ_{cor} = 40 μS/m) to the corona radius r_c. The statistical inception delay and streamer development process are simply ignored. The corona radius r_c is obtained, using analytical expression (2) based on E_c (0.5 or 1.5 MV/m) and the FDTD-computed charge per unit length (q). Then, the conductivity of the cells located within r_c is set to σ_{cor} = 40 μS/m.

$$E_c = \frac{q}{2\pi\varepsilon_0 r_c} + \frac{q}{2\pi\varepsilon_0(2h - r_c)} [\text{V/m}] \tag{2}$$

Equation (2), which is an approximation valid for $r_c \ll h$, gives the electric field at distance r_c below an infinitely long, horizontal uniform line charge +q [C/m], located at height h above flat perfectly conducting ground.

Simulation of corona discharge implemented in the FDTD procedure is summarized below.

If the FDTD-computed electric-field, $E_{zb}{}^n$, at time step n and at a point located below and closest to the wire (at 0.5Δz from the wire axis shown in Fig. 3(a)), exceeds 0.46E_0, where E_0 is given by Eq. (1), the conductivity of σ_{cor} = 40 μS/m is assigned to x- and z-directed sides of the four cells closest to the wire. Note that $E_{zb}{}^n$ is almost the same as $E_{xl}{}^n$ and $E_{xr}{}^n$ at points located to the left and to the right of the wire, respectively, and closest to the wire (at 0.5Δx from the wire axis) (the difference is less than 1%). Therefore, we monitor

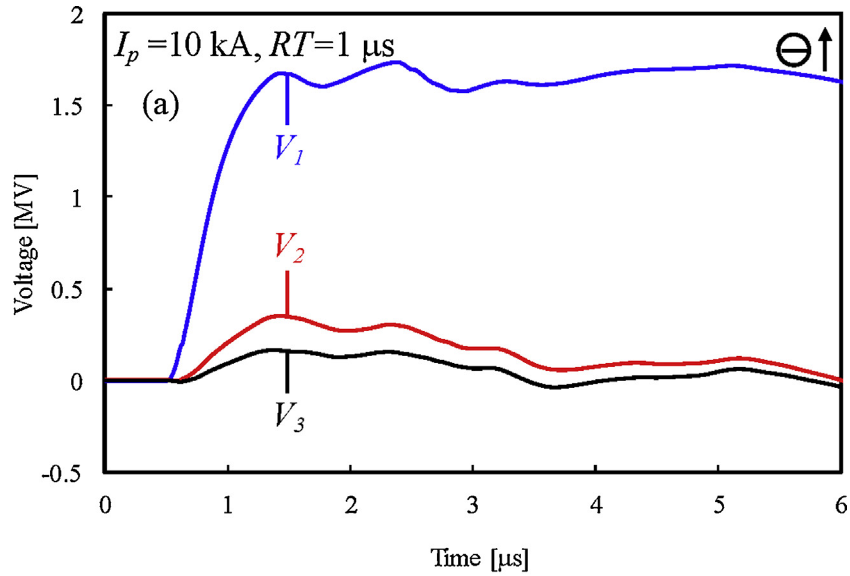

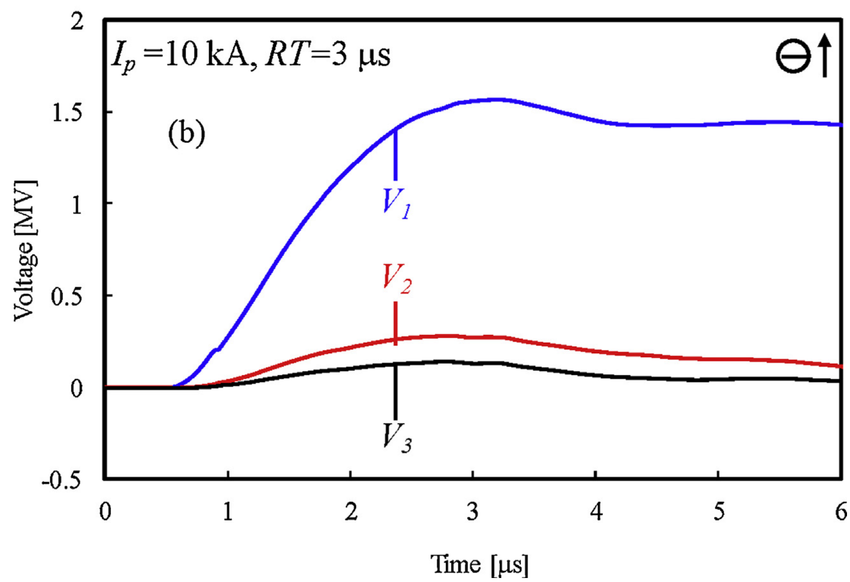

Fig. 6. FDTD-computed (for σ_{cor} = 40 μS/m, E_0 = 2.5 MV/m, and E_{cp} = 0.5 MV/m) waveforms of upper-, middle-, and lower phase transient voltages (V_1, V_2, and V_3, respectively) at the middle tower for a 10-kA positive lightning (negative charge moving up) with a current risetime of (a) 1 μs and (b) 3 μs.

$E_{zb}{}^n$ only for determining the initiation of corona discharge. Also note that neither computed radial corona current nor q–V curves change even if the same conductivity is assigned to y-directed (axial direction) sides of the four cells.

The radial current I^n per unit length of the wire at $y = j\Delta y$ from the excitation point at time step n is evaluated by numerically integrating radial conduction and displacement current densities as follows.

$$I^n(j\Delta y) = \sigma\left[\left(E^n_{xl} + E^n_{xr}\right)\Delta z + \left(E^n_{za} + E^n_{zb}\right)\Delta x\right]\Delta y + \varepsilon_0\left[\begin{array}{l}\left(\dfrac{E^n_{xl} - E^{n-1}_{xl}}{\Delta t} + \dfrac{E^n_{xr} - E^{n-1}_{xr}}{\Delta t}\right)\Delta z\\ + \left(\dfrac{E^n_{za} - E^{n-1}_{za}}{\Delta t} + \dfrac{E^n_{zb} - E^{n-1}_{zb}}{\Delta t}\right)\Delta x\end{array}\right]\Delta y \quad (3)$$

where E_{xl}, E_{xr}, E_{za}, and E_{zb} are radial electric fields closest to the wire shown in Fig. 3(b). The total charge (charge deposited on the wire and emanated corona charge) per unit length of the wire at $y = j\Delta y$ from the excitation point at time step n is calculated as follows.

$$q^n(j\Delta y) = q^{n-1}(j\Delta y) + \frac{I^{n-1}(j\Delta y) + I^n(j\Delta y)}{2}\Delta t \quad (4)$$

Based on q^n given by Eq. (4) and E_c, the corona radius $r_c{}^{n+1}$ at time step $n+1$ is calculated using Eq. (2). The conductivity of σ_{cor} = 40 μS/m is assigned to x- and z-directed sides of all cells located within $r_c{}^{n+1}$. In our model, the corona radius for each meter along the overhead wire is calculated at each time step. As a result, the corona radius has a nonuniform distribution along the conductor. More details on our corona model can be found in [1,2,4].

3. Analysis and results

Fig. 4(a) and (b) shows the waveforms of injected negative lightning return-stroke current (positive charge moving up) current. The peak of the injected lightning current is 10 kA with (a) a risetime of 1 μs and time to half-peak value of about 35 μs and (b) a risetime

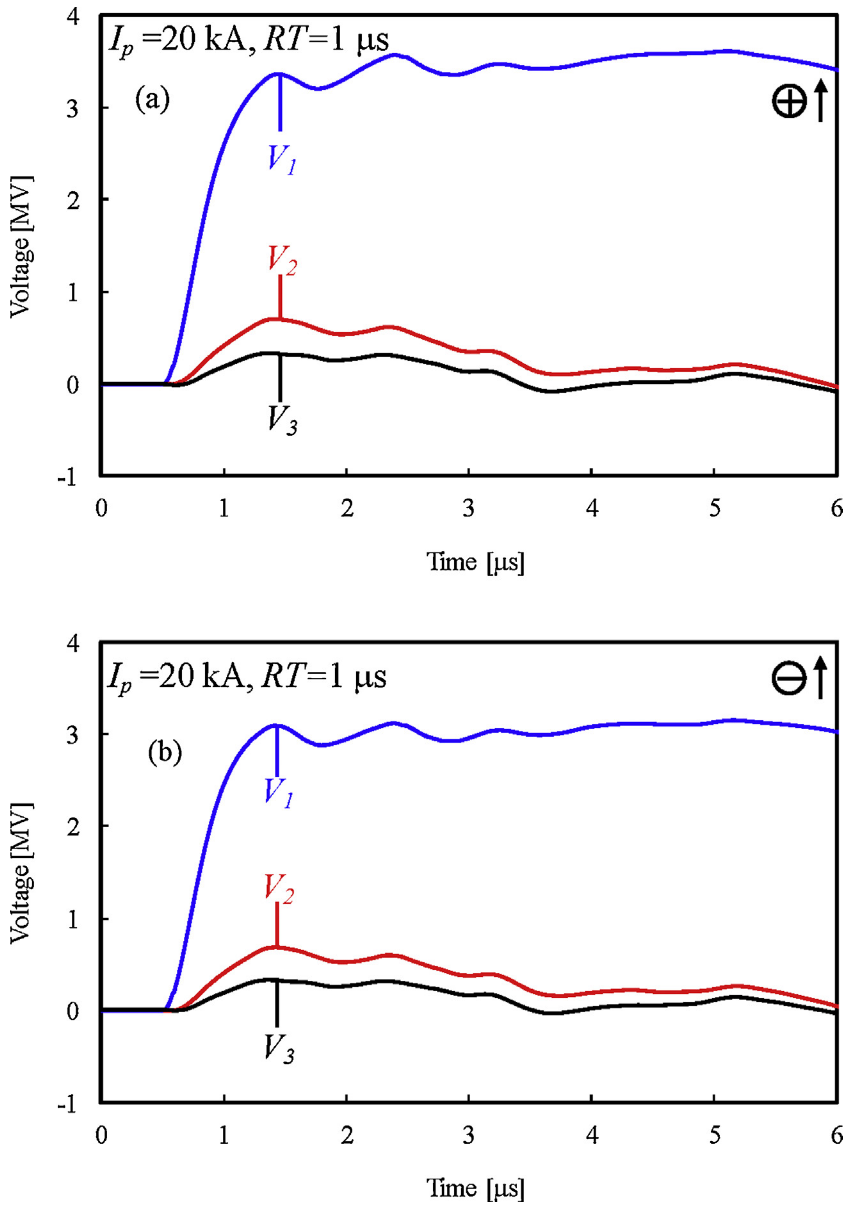

Fig. 7. FDTD-computed (for σ_{cor} = 40 μS/m, E_0 = 2.5 MV/m, E_{cn} = 1.5 MV/m, and E_{cp} = 0.5 MV/m) waveforms of upper-, middle-, and lower phase transient voltages (V_1, V_2, and V_3, respectively) at the middle tower for a 20-kA-peak current with a risetime of 1 μs (a) negative lightning (positive charge moving up) and (b) positive lightning (negative charge moving up).

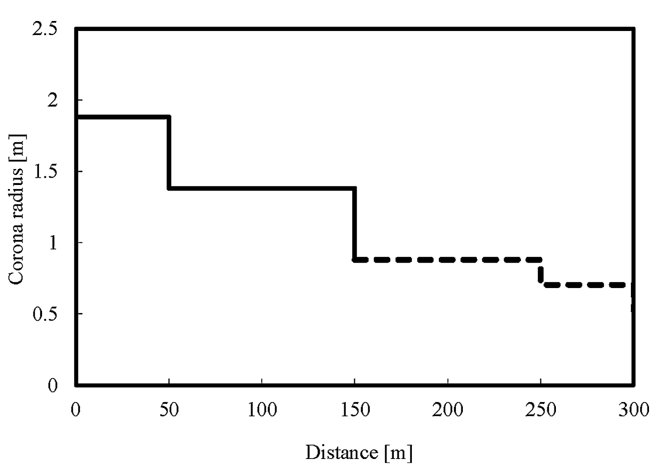

Fig. 8. Variation of corona radius with distance from the lightning strike point (d = 0 m) at time 1 μs. The computations were performed for a 20-kA-peak positive current with a risetime of 1 μs. See text for details.

Table 1
Maximum radii (in meters) of corona emanated from the upper-phase conductor at the lightning strike point.

Stroke polarity	Positive				Negative			
Current peak	10 kA		20 kA		10 kA		20 kA	
Current risetime	1 μs	3 μs	1 μs	3 μs	1 μs	3 μs	1 μs	3 μs
Corona radius	0.84	0.70	1.88	1.38	0.26	0.18	0.53	0.44

Table 2
Peaks of transient voltages at the tower in percent of those in the absence of upper-phase-conductor corona.

Stroke polarity	Positive				Negative			
Current peak	10 kA		20 kA		10 kA		20 kA	
Current risetime	1 μs	3 μs	1 μs	3 μs	1 μs	3 μs	1 μs	3 μs
Upper phase	74	79	68	75	82	87	78	85
Middle phase	97	97	94	96	99	99	99	99
Lower phase	98	97	95	96	99	99	99	99

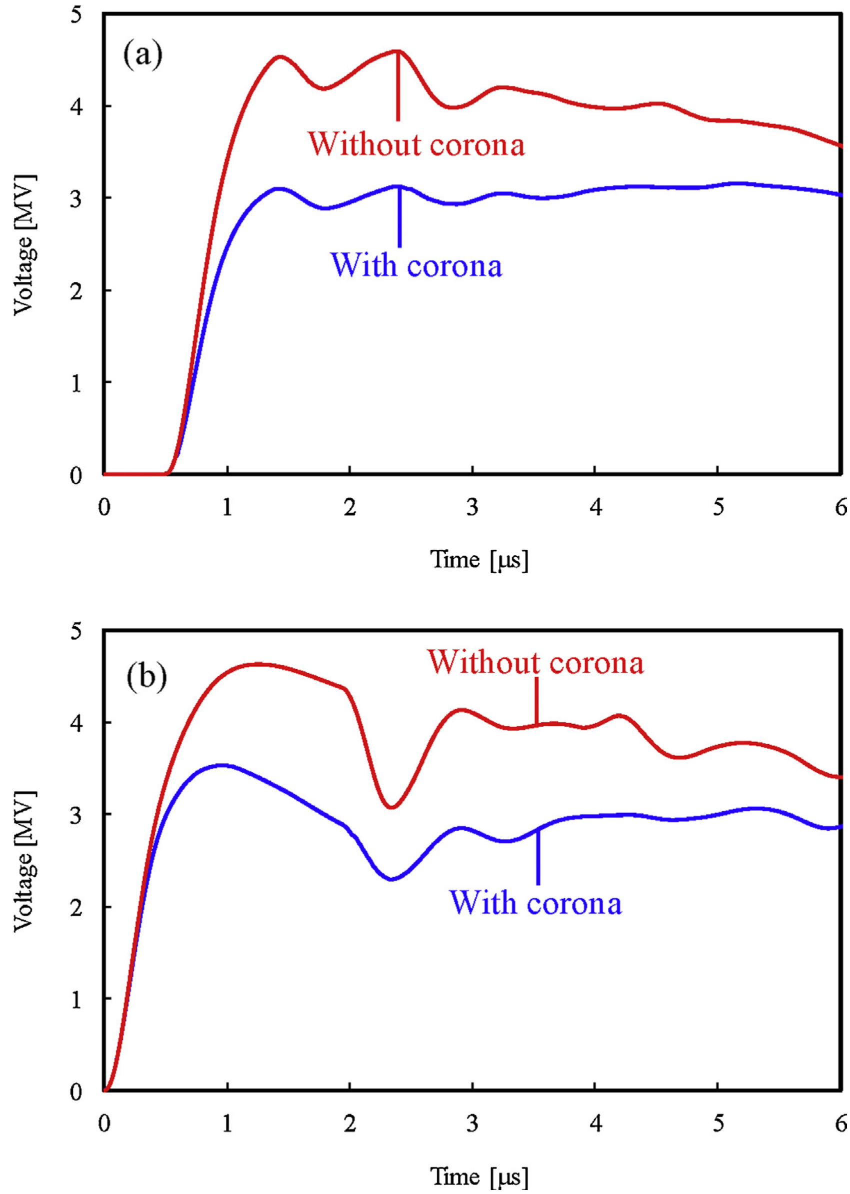

Fig. 9. FDTD-computed waveforms of upper-phase transient voltage at the middle tower with and without corona for a 20-kA positive lightning (negative charge moving up) with a current risetime of 1 μs. The computations were performed for direct lightning strikes to the upper phase conductor (a) at the midpoint of the span and (b) at the point close to the middle tower, respectively.

of 3 μs and time to half-peak value of about 40 μs. Additionally, injected current waveforms with a peak of 20 kA and the same waveshape parameters were used in the simulations, although the corresponding current waveforms are not shown here. Note that corona is considered only on the upper-phase conductor, on which the lightning channel terminates, as shown in Fig. 1(a).

Figs. 5 and 6 show, for negative and positive lightning strokes, respectively, waveforms of transient voltage at the middle tower of the 40-m high transmission line, computed using the FDTD method for a 10-kA current peak with risetimes of (a) 1 μs and (b) 3 μs.

Similarly, but for a 20-kA-peak injected lightning current with a current risetime of 1 μs, Fig. 7(a) and (b) shows waveforms of transient voltage at the middle tower for negative and positive lightning strokes, respectively.

It follows from Figs. 5–7 that the computed transient voltages on the upper phase conductor exceed the typical insulation level for 66/77 kV lines (about 600 kV) and, hence, a flashover will occur in each case.

Fig. 8 shows the variation of corona radius along the upper phase conductor at time 1 μs, computed using the FDTD method for a 20-kA-peak positive current with a risetime of 1 μs at different distances d = 0, 50, 100, 150, 200, 250 and 300 m along the upper-phase conductor from the lightning strike point. As shown in Fig. 8, the radius of corona on the upper phase conductor decreases with distance from the lightning strike point, from 1.88 m at d = 0 m to 0.88 m at d = 150 m. Therefore, the clearance between the tower and conductor with corona is 1.12 m. For typical insulation (about 600 kV), a mid-span strike will cause an insulator flashover at 150 m (at the nearest tower). Thus, the corona radius versus distance dependence is meaningful only up to 150 m from the strike point, and the results for d > 150 m (broken line in Fig. 8) correspond to the case of ideal (considerably-higher-level) insulation. Note that corona radius variation is step-like due to the size of square or rectangular cells employed in the FDTD computations.

Table 1 summarizes maximum corona radii for different stroke polarities, current magnitudes, and current risetimes. Maximum

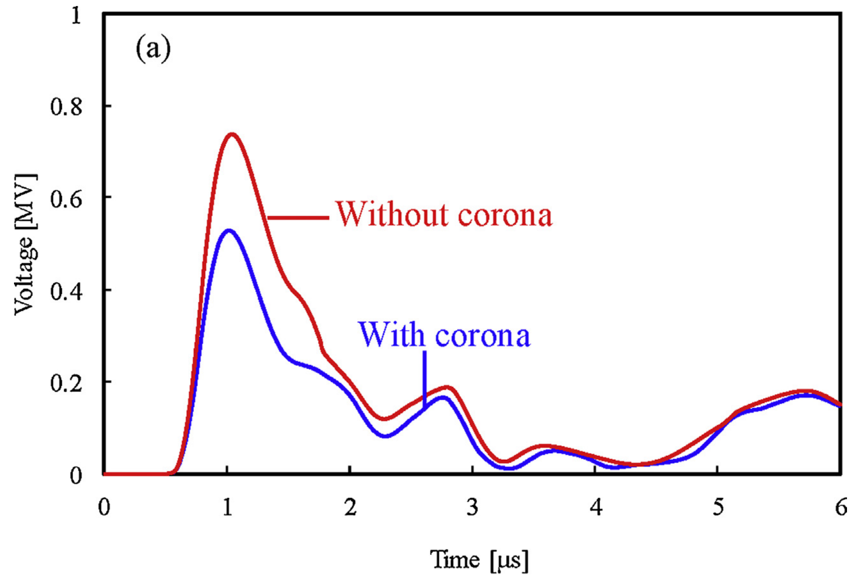

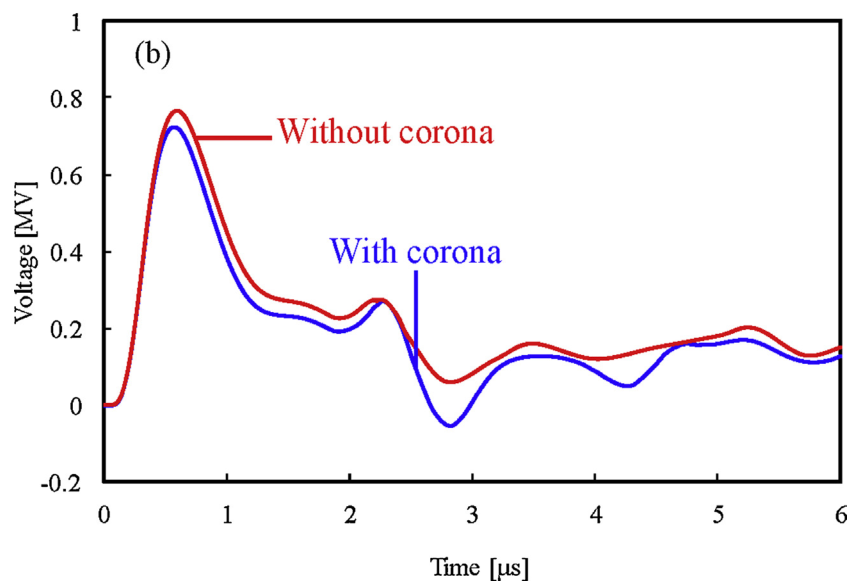

Fig. 10. FDTD-computed waveforms of upper-phase transient voltage at the middle tower with and without corona for a 20-kA positive lightning (negative charge moving up) with a current risetime of 1 μs. The computations were performed for direct lightning strikes to the ground wire (a) at the midpoint of the span and (b) at the top of the middle tower, respectively.

corona radii for negative-stroke cases with 10-kA current peak and current risetimes of 1 μs and 3 μs are 0.26 m and 0.18 m, and those for positive-stroke cases are 0.84 m and 0.7 m, respectively. For a 20-kA peak current, maximum corona radii are 0.53 m and 0.44 m for negative-stroke cases, and those for positive-stroke cases are 1.88 m and 1.38 m, for risetimes of 1 μs and 3 μs. Note that in a negative stroke positive charge moves up along the channel (negative charge is injected into the system) and in a positive stroke the situation is reversed.

Table 2 summarizes peaks of transient voltages at the tower in percent of those in the absence of upper-phase-conductor corona for all three phases and different injected currents. It follows from Table 2 that, as expected, the reduction of transient-voltage peak due to corona is more significant for the upper phase

Table 3
Peaks of transient voltages at the tower in percent of those in the absence of corona for positive strokes with 20-kA-peak and 1-μs-risetime current and different stroke locations.

Stroke locations	Upper phase conductor		Ground wire	
	Midpoint of the span	Close to the middle tower	Midpoint of the span	Top of the middle tower
Upper phase	68	76	72	94
Middle phase	94	95	76	95
Lower phase	95	96	80	96

conductor struck by lightning. For a 10-kA peak current, the upper-phase-conductor voltage peaks are reduced by 26% and 21% for a positive-stroke with 1-μs-risetime and 3-μs-risetime currents, respectively, and those for negative-stroke are reduced by 18% and 13%, respectively. For a 20-kA peak current, the corresponding upper-phase-voltage peaks are reduced by 32% and 25% for positive-stroke case, and those for negative-stroke case are reduced by 22% and 15%.

The reason why the transient voltage at the tower for the upper-phase conductor is reduced is the reduction of its characteristic impedance by corona. Transient voltages of the other two phases are less influenced by corona on the upper-phase conductor because the reduction of the (inducing) upper-phase voltage is counteracted by the increase of coupling from the upper-phase conductor.

4. Discussion

We now compare our results with those for other configurations, including lightning strikes to the overhead ground wire and to the phase conductor near the middle tower.

Fig. 9(a) and (b) shows FDTD-computed waveforms of transient voltages at the middle tower with and without upper-phase-conductor corona for direct lightning strikes to the upper phase conductor at the mid-span point and at the point close to the middle tower, respectively. A positive stroke with 20-kA current peak and current risetime of 1 μs is employed. For both strike locations, the upper-phase transient voltage is reduced by about 30%. This reduction is caused by the decrease of characteristic impedance of the upper-phase conductor due to corona. Even when the strike point is the midpoint of the span, the upper-phase insulator transient voltage decreases. This is because the phase-conductor voltage near the strike point decreases due to the corona and the resultant reduced (relative to the case without corona) voltage surge propagates to the tower.

Table 3 (columns 2 and 3) shows peaks of transient voltages at the tower in the presence of upper-phase-conductor corona in percent of those in the absence of corona. Fig. 10(a) and (b) shows FDTD-computed waveforms of transient voltages at the tower with and without ground-wire corona for direct lightning strikes to the ground wire at the midpoint of the span and at the top of the middle tower, respectively. A positive stroke with 20-kA current peak and current risetime of 1 μs is employed. Note that corona is considered only on the ground wire in these simulations.

Table 3 (columns 4 and 5) shows peaks of transient voltages at the tower in the presence of ground-wire corona in percent of those in the absence of corona. For the direct lightning strike to the top of the middle tower, the reduction of each transient voltage is about 5%. This is because the negative reflection from the tower base returns to the tower top in about 0.27 μs, and suppresses the increase of tower-top and ground-wire voltage, which results in a relatively small corona extent around the ground wire. On the other hand, for the direct lightning strike to the ground wire at the midpoint of the span, the reduction of each transient voltage is about 20 to 30%. This is because the negative reflections from the tower bases return to the strike point in about 1.3 μs, allowing a larger corona expansion on the ground wire near the strike point, which increases coupling to phase conductors and decreases transient voltages at the tower (e.g., Thang et al. [4]). In our simulations, a personal computer with an OS of 64-bit Windows 7 and a CPU of 3.46-GHz Intel Core I7 was used. The time increment was set to $\Delta t = 0.047$ ns, and the maximum observation time was set to 6 μs. The computation time needed for one run was about 80 h, and the memory required was 3.8 GB.

5. Conclusions

We have applied the simplified model of corona discharge proposed for FDTD computations to simulation of transient voltages at the tower of 40-m-high transmission line for the case of direct lightning strikes to an upper phase conductor. The FDTD-computed transient voltages are reduced by corona discharge on the upper phase conductor. However, the upper-phase-voltage peaks are reduced by only 26% and 21% for a positive-stroke with 1-μs-risetime and 3-μs-risetime currents, respectively, and those for negative-stroke are reduced by 18% and 13%, respectively. For a 20-kA peak current, the corresponding upper-phase-voltage peaks are reduced by 32% and 25% for the positive-stroke case, and those for the negative-stroke case are reduced by 22% and 15%. Whether with or without corona, the computed voltages on the top (struck) phase conductor are in the megavolts range, considerably higher than the typical insulation level (about 600 kV) of 66/77 kV lines. Thus, although the corona effect does reduce the conductor voltage, this reduction cannot prevent the line flashover.

References

[1] T.H. Thang, Y. Baba, N. Nagaoka, A. Ametani, J. Takami, S. Okabe, V.A. Rakov, A simplified model of corona discharge on overhead wire for FDTD computations, IEEE Trans. Electromagn. Compat. 54 (Jun (3)) (2012) 585–593.
[2] T.H. Thang, Y. Baba, N. Nagaoka, A. Ametani, J. Takami, S. Okabe, V.A. Rakov, FDTD simulation of lightning surges on overhead wires in the presence of corona discharge, IEEE Trans. Electromagn. Compat. 54 (Dec (6)) (2012) 1234–1243.
[3] K.S. Yee, Numerical solution of initial boundary value problems involving Maxwell's equations in isotropic media, IEEE Trans. Antennas Propag. 14 (May (3)) (1966) 302–307.
[4] T.H. Thang, Y. Baba, N. Nagaoka, A. Ametani, N. Itamoto, V.A. Rakov, FDTD simulation of insulator voltages at a lightning-struck tower considering ground-wire corona, IEEE Trans. Power Delivery 28 (Jul (3)) (2013) 1635–1642.
[5] T. Noda, Development of a Transmission-Line Model Considering the Skin and Corona effects for Power System Transient Analysis, Doshisha University, 1996, Ph.D. Thesis.
[6] T. Noda, T. Ono, H. Matsubara, H. Motoyama, S. Sekioka, A. Ametani, Charge–voltage curves of surge corona on transmission lines: two measurement methods, IEEE Trans. Power Delivery 18 (1) (2003) 307–314.
[7] A. Inoue, Study on propagation characteristics of high-voltage traveling waves with corona discharge CRIEPI Report, 114, 1983 (in Japanese).
[8] C.F. Wagner, I.W. Gross, B.L. Lloyd, High-voltage impulse tests on transmission lines, AIEE Trans. Power Apparatus Syst. 73 (Apr) (1954) 196–210.
[9] Y. Baba, V.A. Rakov, Applications of the FDTD method to lightning electromagnetic pulse and surge simulations, IEEE Trans. Electromagn. Compat. 56 (Dec (6)) (2014) 1506–1521.
[10] Y. Baba, V.A. Rakov, On the transmission line model for lightning return stroke representation, Geophys. Res. Lett. 30 (Dec (24)) (2003) 4.
[11] Z.P. Liao, H.L. Wong, B.P. Yang, Y.F. Yuan, A transmission boundary for transient wave analysis, Sci. Sin. A27 (10) (1984) 1063–1076.
[12] T. Noda, S. Yokoyama, Thin wire representation in finite difference time domain surge simulation, IEEE Trans. Power Delivery 17 (Jul (3)) (2002) 840–847.
[13] G. Hartmann, Theoretical evaluation of Peek's law, IEEE Trans. Ind. Appl. 20 (Nov (6)) (1984) 1647–1651.
[14] V. Cooray, The Lightning Flash, The Institution of Electrical Engineers, UK, 2003, pp. 79, 570 pages.
[15] R.T. Waters, D.M. German, A.E. Davies, N. Harid, H.S.B. Eloyyan, Twin conductor surge corona, in: Paper presented at the Fifth Int. Symp. High Voltage Engineering, Braunschweig, Federal Republic of Germany, 1987.